

IFSCC 2025 Congress 2025, Full Paper (IFSCC 2025-651)

Electrokinetic Analysis Reveals Common Conditioner Ingredient Interactions with Human Hair

Huijun Phoebe Tham ¹, Kah Yuen Yip ¹, Thomas Luxbacher ², Roger L. McMullen ³ and Thomas L. Dawson Jr. ^{4,5*}

¹ A*STAR Skin Research Labs (A*SRL), Agency for Science, Technology and Research (A*STAR), 11 Mandalay Rd, #17-01, Singapore 308232, Republic of Singapore; ² Anton Paar GmbH, Anton-Paar-Strasse 20, 8054 Graz, Austria; ³ Ashland Specialty Ingredients, G.P., 1005 US HWY 202/206, Bridgewater, New Jersey 08807, USA; ⁴ Center for Cell Death, Injury Regeneration, Departments of Drug Discovery Biomedical Sciences and Biochemistry Molecular Biology, Medical University of South Carolina, Charleston, SC, USA; ⁵ A*STAR Skin Research Labs (A*SRL), Agency for Science, Technology and Research (A*STAR) & Skin Research Institute of Singapore (SRIS), 11 Mandalay Rd, #17-01, Singapore 308232, Republic of Singapore

1. Introduction

Hair conditioners incorporate diverse actives—cationic surfactants, humectants, emollients, and silicones—to condition, moisturize, and protect hair by reducing inter-fibre friction [1-3]. Cationic surfactants, with positively charged quaternary ammonium groups, neutralize the hair's negative charge, enabling detangling and cuticle smoothing [1, 3, 4]. Humectants retain moisture, emollients reduce friction via lubrication, and silicones form protective films that enhances shine and reduces frizz [3]. Effective conditioning requires preferential binding of actives to the hair surface[1]. Polyquaterniums, cationic polymers with high molecular weight, exhibit stronger binding than monomeric surfactants due to polyelectrolyte-surfactant complex formation [1, 3, 5]. However, their reduced hydrophilicity and resistance to rinsing can lead to buildup [2, 6]. Substantivity correlates with molecular weight – molecules with higher molecular weights partition more readily to the hair's hydrophobic F-layer via dispersion forces and entropy effects [2, 7, 8]. In contrast, aliphatic quaternary ammonium compounds e.g. hexadecyltrimethylammonium chloride (CTAC), behentrimonium chloride (BTMC), behentrimonium methosulfate (BTMS), and stearylalkonium chloride (STAC), rely on electrostatic interactions facilitated by hair's low isoelectric point (IEP) [9-11]. Their smaller size avoids film formation, minimizing buildup while their alkyl chains enhance binding via hydrophobic interactions, though lesser than polyquaterniums [12].

Quantifying surfactant deposition remains challenging. Techniques like Inductively Coupled Plasma Optical Emission Spectroscopy (ICP-OES) [13], Time-of-Flight Secondary Ion Mass Spectrometry (ToF-SIMS) [13], X-Ray Fluorescence spectroscopy (XRF) [14] and Atomic

Force Microscopy [15] lack kinetic resolution or struggle with hydrocarbon detection. Dissipative quartz crystal microbalance (D-QCM) and ellipsometry are restricted to flat substrates [16], while hair's fibrous, heterogeneous structure introduces variability.

The deposition efficacy of four aliphatic cationic surfactants (BTMC, BTMS, CTAC, STAC) on healthy and damaged hair was assessed using streaming potential [17] – a method capable of *in situ* kinetic analysis on fibrous substrates. Wet combing assesses functional outcomes, while silicon oxide wafers validated adsorption trends by eliminating biological variability.

2. Materials and Methods

Conditioner formulations: Four formulations were prepared with 1% cationic surfactant, fatty alcohol mixture, emulsifier, preservative, and deionized water (Table 1).

Table 1. Evaluated hair conditioner formulations.

Ingredient	Conditioner #1	Conditioner #2	Conditioner #3	Conditioner #4
Cetyl/stearyl alcohol	4 g	4 g	4 g	4 g
Emulsifier	2 g	2 g	2 g	2 g
Cationic surfactant	1.18 g BTMC (85%)	2 g BTMS (50%)	1 g CTAC	1 g STAC
Preservative	1 g	1 g	1 g	1 g
Deionized water	91.82 g	91 g	92 g	92 g
Total	100 g	100 g	100 g	100 g

The aqueous phase containing cationic surfactant and deionized water, and the oil phase containing cetyl/stearyl alcohol and emulsifier, were separately heated to 70 °C under stirring. The melted oil phase was combined with the aqueous phase at 70 °C, homogenized, and cooled. Preservative was added during cooling.

Hair tresses: Healthy and bleached damaged Asian Black Remy hair tresses (8 inches long) were cleaned with 1% sodium dodecyl sulfate (SDS), rinsed, air-dried, and bundled into 1 g samples. Damaged hair was prepared by bleaching with hydrogen peroxide and done by the vendor. Prior to use, all hair samples were thoroughly cleaned with and rinsed extensively.

Silicon wafer: A silicon wafer (thickness 0.7 mm) with a silicon oxide coating (1000 Å) was cut into 20 mm x 10 mm pieces (Si | SiO₂), ultrasonically cleaned with isopropyl alcohol and ultrapure water, and dried at 50 °C.

Zeta (ζ) potential analyses: The ζ -potential of hair and silicon wafer pieces were measured using a solid-state electrokinetic analyser after 15-minute buffer equilibration. An electrolyte buffer solution was first prepared using 0.9 mM potassium chloride (KCl), 1 mM sodium hydrogen phosphate (Na₂HPO₄), and 0.2 mM potassium dihydrogen phosphate (KH₂PO₄). ζ -potential is calculated from the slope of streaming potential (U_{str}) with varying differential pressure ($d\Delta P$) using the classic Smoluchowski formula [18]. Normalised ζ values were calculated by taking ζ divided by the initial ζ -potential of the sample (ζ_0).

Adsorption kinetics were recorded in dynamic mode at a time resolution of 160 ms, providing real-time adsorption/desorption processes. U_{str} was converted to ζ -potential using the approximated Helmholtz-Smoluchowski formula (Equation 1) below:

$$\zeta = \frac{dU_{str}}{d\Delta P} \frac{\eta}{\epsilon_0 \epsilon_r} \kappa_B - \text{Equation 1}$$

where ϵ_0 is the vacuum permittivity, ϵ_r , η and κ_B are the dielectric constant, the electrolyte viscosity and the conductivity, respectively.

ζ vs. Concentration: Fresh buffer solutions containing conditioner were incrementally added to the electrolyte, up to 1000 ppm for hair and 250 ppm for wafers. U_{str} values were recorded at each equilibrium point.

ζ vs. Time: For both hair and wafer samples, after baseline stabilization, 250 ppm conditioner was introduced for 2400 s. U_{str} values were converted to ζ -potential using Equation 1 and plotted against time. Clean buffer solution was used for rinsing.

ζ vs. pH: For hair, a pea-sized (~0.5 cm) amount of each conditioner was coated on a 1 g wet hair switch for 2 minutes, excess conditioner was rinsed off. For wafers, the analyses were conducted after 250 ppm was added through the machine. The ζ -pH dependence and IEP were determined via automated pH scans (0.3 pH increments, 0.05 M hydrochloric acid (HCl)). ζ values at each pH was measured in quadruplicate, starting from the native pH of the phosphate buffer and titrated to lower pH values.

Wet combing: European hair tresses (10 g, 18 cm) were bleached in two regions defined by an acrylic frame (Figure 1a), and quantified using integrated force curves (Figure 1b). Two tresses were measured five times each. Commercial bleach was used, followed by shampooing twice with 3% (w/w) sodium laureth sulphate (SLES):cocamidopropyl betaine (CAPB) (12:2). After bleaching, the entire hair tress was treated with 1 g conditioner. Wet combing measurements were performed both post-bleaching vs. post-treatment.

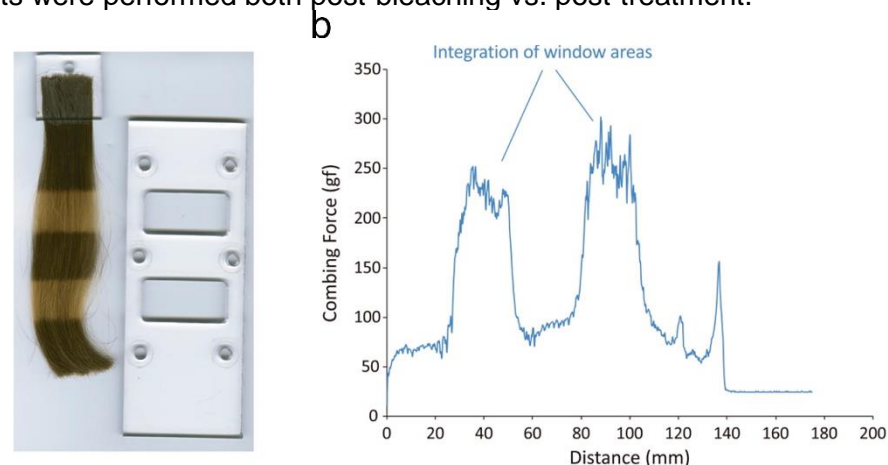


Figure 1. a) Photograph of a hair tress after bleaching with a window treatment frame. b) Wet combing curve of hair after the bleaching treatment.

Attenuated Total Reflectance Fourier Transform Infrared (ATR-FTIR): Three different tresses per conditioner group were scanned at three different locations each (8 cm^{-1} , 16 scans, $4000 - 650\text{ cm}^{-1}$). The absorbance peak at 1040 cm^{-1} was normalised to Amide I ($\text{ca. } 1650\text{ cm}^{-1}$).

3. Results

Both healthy and damaged hair displayed negative ζ -potential at the intrinsic pH of the buffer solution (pH~7.5), consistent with their inherent surface charge ($\zeta_{\text{healthy}} = -29.2 \pm 3.9\text{ mV}$; $\zeta_{\text{damaged}} = -0.9 \pm 0.2\text{ mV}$), which aligned with previous reports [19]. Contrary to expectations – where bleaching-induced oxidation of cystine disulfide bonds to sulfonic acid groups should amplify negative charge – damaged hair exhibited a less negative zeta potential. This discrepancy highlights multifaceted alterations in hair surface properties post-bleaching. Firstly, the

introduction of strongly acidic surface groups enhances hydrophilicity, which correlates with diminished ζ -potential magnitude [20, 21]. Secondly, increased hydrophilicity and structural damage promote water penetration into the hair fibre, introducing ionic conductance unaccounted for by the Smoluchowski model. This leads to underestimation of the true ζ -potential, resulting in an apparent ζ -potential (ζ_{app}). Lastly, fibre swelling in damaged hair blurs the solid-liquid interface, creating a diffuse transition zone that attenuates the streaming potential signal and distorts measurements [22].

Adsorption on healthy and damaged hair (ζ vs. Concentration)

Conditioners #1 – #4 (1% BTMC, BTMS, CTAC and STAC respectively), were applied to healthy and damaged hair, with normalised ζ -potential shown in Figure 2.

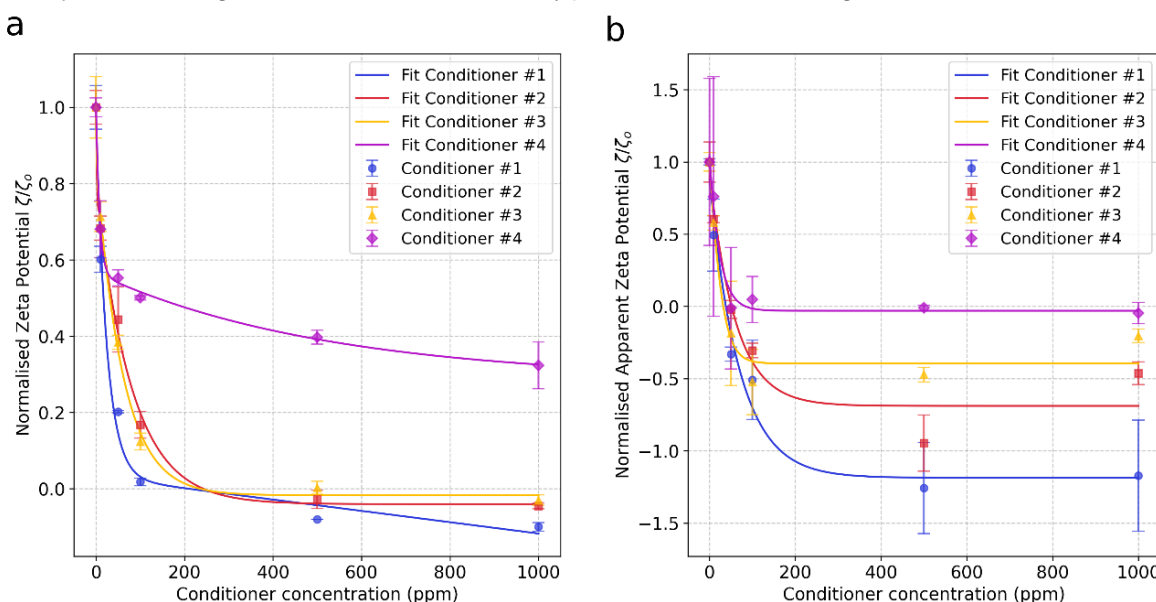


Figure 2. Changes in normalised zeta potential with increasing conditioner concentration added to a) healthy hair, and b) damaged hair.

For both healthy and damaged hair, Conditioner #1 induced the largest ζ -shift, while Conditioner #4 showed minimal deposition due to STAC's bulky aromatic group causing steric hindrance (Figure 2). On healthy hair, Conditioners #1 and #4 did not reach saturation at 1000 ppm, whereas Conditioners #2 and #3 equilibrated at ~500 ppm. Damaged hair saturated at lower concentrations (≤ 500 ppm), reflecting fewer available binding sites despite its higher negative charge [23]. Charge reversal occurred at 50 – 150 ppm on damaged hair for all conditioners, but only Conditioners #1 - #3 achieved this on healthy hair. Post-reversal, further deposition has to rely on hydrophobic interactions (weaker for CTAC's shorter C16 chain), while STAC's steric bulk inhibited bilayer formation.

Adsorption and pH dependence (ζ vs. pH)

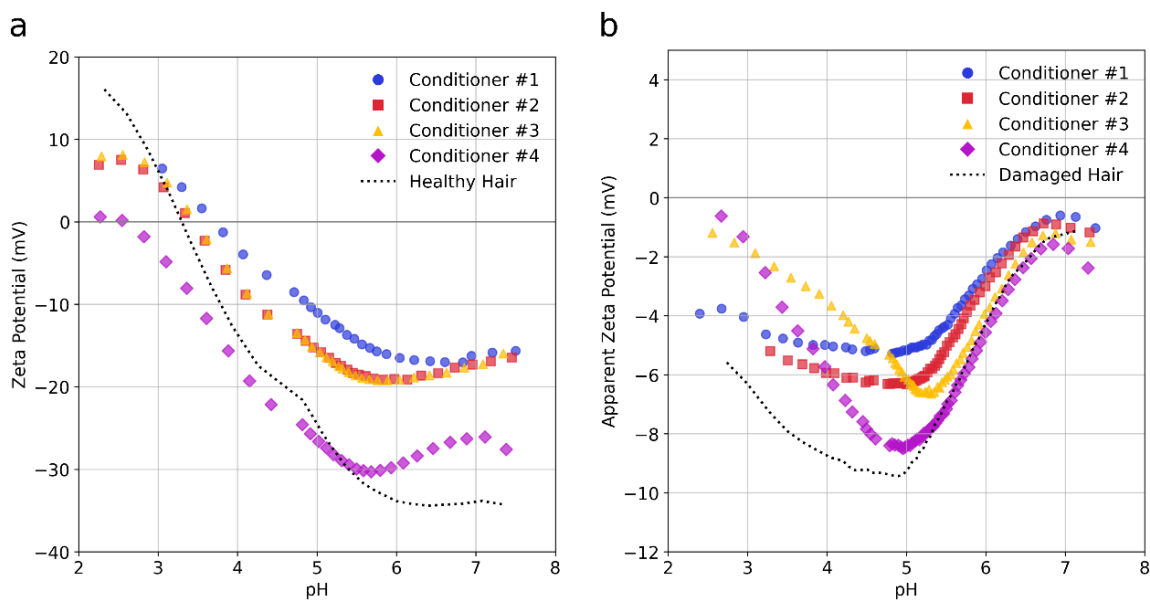


Figure 3. ζ -pH curves for a) healthy and b) damaged hair applied with conditioners by hand.

Post-treatment ζ -potentials shifted upward across all pH values while maintaining a similar curve shape (Figure 3), with the shift magnitude increasing in order of Conditioner #4 < #3 \approx #2 < #1, similar to Figure 2. Healthy hair IEPs followed a similar order: Conditioner #4 (2.58) < #2 (3.42) \approx #3 (3.47) < #1 (3.70). Considering an uncertainty of ± 0.2 pH, the effects of Conditioners #2 and #3 at equilibrium cannot be distinguished. Higher IEPs indicate cationic surfactant coating reduced negative charge, requiring less H⁺ for neutralization. Conditioner #4's lower IEP (2.58) compared to healthy hair (3.31) suggests that, despite the low levels of cationic STAC remaining on the surface, other residual non-surfactant adsorbates (e.g., formulation additives) remained. The residual adsorbates' effect are also visible at higher pH values (>5.5), indicating Conditioner #4 was not completely removed by rinsing. All conditioners induced mild swelling near pH 5.5, which was absent in untreated hair. For damaged hair, ζ -potential shifts at neutral pH were smaller, with Conditioner #4 showing the least change. The pH 5 swelling minimum in untreated damaged hair diminished post-treatment, particularly with Conditioners #1 and #2), indicating reduced water penetration due to surface coating. No IEP was reached for damaged hair under any condition.

Adsorption and desorption dynamics (ζ vs. Time)

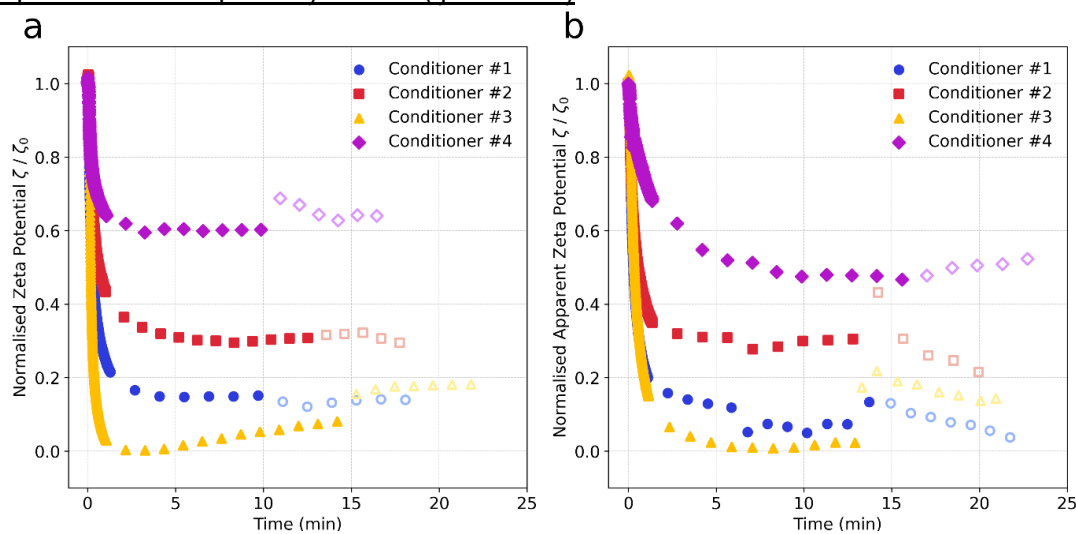


Figure 4. Normalised sorption kinetics of a) healthy hair, and b) damaged hair when the four conditioners (250 ppm) were added and upon rinsing. Filled markers represent adsorption data, empty markers represent desorption data. Conditioners were added at $t = 0$.

Generally, all conditioners reached equilibrium within 5 minutes (Figure 4). Conditioner #4 caused the smallest ζ -shift for both healthy and damaged hair, while #3 (CTAC) adsorbed faster than #1 and #2 due to its shorter C16 chain enhancing diffusivity [24]. However, CTAC's weaker van der Waals interactions led to gradual desorption even in the deposition stage, particularly on healthy hair (Figure 4a). During rinsing, Conditioners #3 and #4 were more easily removed from both hair types, attributed to shorter alkyl chains reducing hydrophobic stabilization [23] in contrast to Conditioners #1 and #2, which were more resistant to disruption of bilayer/multilayer structures by rinsing shear forces. No apparent charge reversal was reached in either healthy or damaged hair upon conditioner addition.

Comparison to a model surface

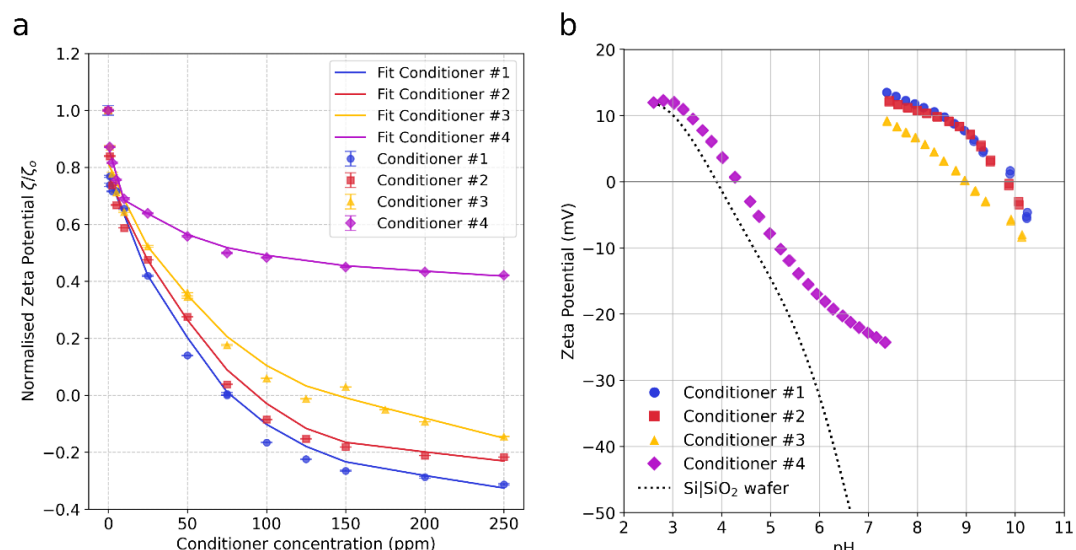


Figure 5. Changes in a) normalised ζ -potential with increasing conditioner concentration and b) ζ -potential changes with pH levels at adsorption equilibrium (250 ppm) on $\text{Si} \mid \text{SiO}_2$ wafers.

To circumvent hair's structural complexity, Si | SiO₂ wafers served as a simplified model for hair's negative surface charge. Despite differences in surface chemistry and area, conditioner adsorption trends on wafers (Figure 5a) mirrored those on healthy/damaged hair (Figure 2). Charge reversal occurred at lower concentrations (75–150 ppm vs. ≈200 ppm for hair), attributed to the wafer's smooth surface (4 cm² vs. hair's ≈342 cm²), enabling efficient adsorption. Higher equilibrium ζ -potentials (wafer: ≈10 mV vs. hair: 0–2 mV) confirmed more complete surface coverage on wafers. IEP shifts post-treatment followed: pristine wafer (3.91) < #4 (4.32) < #3 (8.99) < #2 (9.84) ≈ #1 (9.98). Conditioners #1 and #2 were indistinguishable at equilibrium given the same ±0.2 pH uncertainty. While #4 showed minimal adsorption versus wafers, ζ -potential divergence at increasing pH values indicated partial STAC retention.

Wet combing

To correlate cationic surfactant deposition with practical conditioning efficacy, wet combing performance was evaluated for treated healthy and damaged hair (Figure 6). Wet combing forces are influenced by fibre swelling, inter-fibre adhesion, and treatment-induced surface tension reduction [25] and combing work difference (post- vs. pre-treatment) serves as the efficacy metric, where higher values indicate better conditioning.

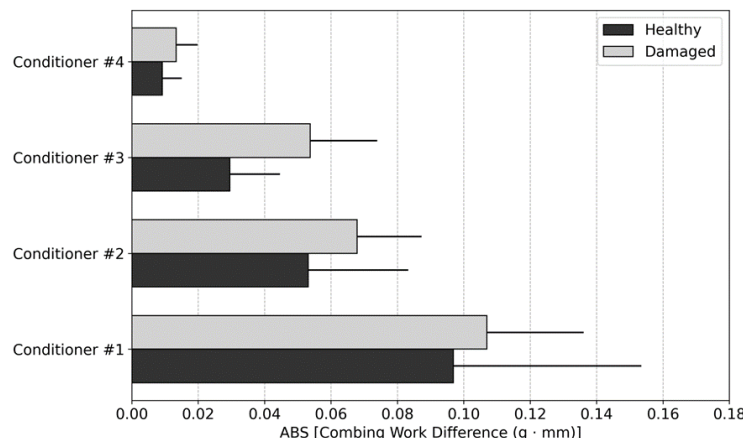


Figure 6. Combing work data (integrated window regions) obtained from wet combing curves for hair treated with various conditioner formulations.

All conditioners reduced combing forces, with efficacy ranking: Conditioner #4 < #3 < #2 < #1. Damaged hair exhibited marginally greater combing work differences than healthy hair across treatments, though statistically insignificant. Conditioner #1 (BTMC) outperformed #2 (BTMS), consistent with streaming potential data. As the key difference between BTMS and BTMC lies only in their counterion, we propose that BTMC's better conditioning is likely due to chloride's smaller size facilitating displacement during adsorption, enhancing effective charge density, and strengthening electrostatic interactions with the hair surface. While electrostatic interactions are the primary driving force for cationic surfactant-hair surface interactions, these interactions are stabilized by van der Waals forces between adjacent long alkyl chains. Longer alkyl chains (e.g., BTMC's C22) enhance the van der Waals interactions [4, 9, 26], while shorter chains (e.g. CTAC (C16), STAC (C18)) have weaker hydrophobic interactions, explaining the reduced combing force reduction observed for Conditioners #3 and #4. CTAC (Conditioner #3)

unexpectedly surpassed STAC (Conditioner #4). This anomaly reflects CTAC's higher deposition levels (evidenced by streaming potential) overriding its shorter chain length, likely due to STAC's aromatic group impeding adsorption through steric hindrance.

Damage assessment by ATR-IR

ATR-IR is often used to measure the hair surface cysteic acid level as an indication of oxidative damage. Bare healthy hair has much lower oxidative damage (2.1 ± 0.1) compared to bare damaged hair (7.2 ± 0.1). Despite improvement in combability and the variation in conditioner deposition there was no appreciable change in cysteic acid levels of healthy and damaged hairs after any conditioner application, clearly indicating that conditioners do not reverse any oxidative damage on hair.

4. Discussion

The adsorption dynamics of cationic surfactants on hair are governed by molecular structure, substrate properties, and formulation interplay. Our results demonstrate that alkyl chain length is pivotal: BTMC (C22) and BTMS (C22) exhibited superior deposition over CTAC (C16) and STAC (C18) due to stronger van der Waals interactions. These interactions stabilize surfactant layers, prolonging residence time and enhancing substantivity [27]. However, counterion dissociation further modulates efficacy. We propose that chloride's smaller size (BTMC) dissociates easily, enabling higher charge density, strengthening electrostatic binding, while methosulfate's hydrophilicity (BTMS) and larger size favors formulation stability over deposition [28]. CTAC (C16) outperformed STAC (C18) despite its shorter chain. This anomaly arises from steric hindrance in STAC's bulky aromatic group, obstructing hair surface alignment. Such structural constraints override chain-length advantages, highlighting molecular geometry's role in adsorption efficiency. Damaged hair introduced complexities: despite higher negative charge (oxidized sulfonic groups), its reduced ζ -potential magnitude reflects swelling-induced ionic conductance and blurred solid-liquid interfaces. These distort streaming potential measurements but damaged hair showed greater combing force reduction. Silicon wafers, while effective for screening surfactant trends, oversimplify hair's heterogeneity, failing to replicate porosity or swelling, limiting translational relevance.

5. Conclusion

This study establishes streaming potential as a critical tool for resolving cationic surfactant adsorption mechanisms on hair. Molecular design dictates performance, where longer alkyl chains enhance substantivity via van der Waals forces, while smaller counterions enhance charge density. Bulky groups reduce efficacy, underscoring the need for structural optimization. There are also practical tradeoffs in designing cationic surfactants, e.g., BTMC's strong adsorption suits intensive repair but risks buildup, whereas CTAC/STAC's rinsability would favour daily use. While silicon wafers offer rapid screening, their limitations necessitate complementary methods for real-world prediction. ATR-IR confirmed conditioners improve surface manageability but do not repair internal damage, emphasizing their role as cosmetic but not therapeutic agents. By bridging molecular interactions to macroscopic outcomes, this work

provides a framework for rational formulation design. Future studies could explore hybrid surfactants or advanced substrates mimicking hair's complexity, further refining predictive models. Streaming potential was proven to be a critical tool for optimizing conditioner efficacy, enabling formulators to balance deposition, stability, and rinsability in product development.

References

- [1] C. Robbins, S.-V. B. Heidelberg, Ed. *Chemical and Physical Behaviour of Human Hair*, 5th ed. 2012.
- [2] M. F. Gavazzoni Dias, "Hair cosmetics: an overview," *Int J Trichology*, vol. 7, no. 1, pp. 2-15, Jan-Mar 2015, doi: 10.4103/0974-7753.153450.
- [3] L. Fernández-Peña and E. Guzmán, "Physicochemical aspects of the performance of hair-conditioning formulations," in *Cosmetics* vol. 7, ed: MDPI AG, 2020, pp. 1-21.
- [4] C. Fernandes, B. Medronho, L. Alves, and M. G. Rasteiro, "On Hair Care Physicochemistry: From Structure and Degradation to Novel Biobased Conditioning Agents," in *Polymers* vol. 15, ed: MDPI, 2023.
- [5] J. Shokri, M. Shamseddini Lori, and F. Monajjemzadeh, "Examining polyquaternium polymers deposition on human excised hair fibers," *Journal of Cosmetic Dermatology*, vol. 17, no. 6, pp. 1225-1232, 2018, doi: <https://doi.org/10.1111/jocd.12454>.
- [6] O. M. Musa and M. A. Tallon, "Hair Care Polymers for Styling and Conditioning," American Chemical Society, 2013, ch. 15, pp. 233-284.
- [7] Hössel, Dieing, Nörenberg, Pfau, and Sander, "Conditioning polymers in today's shampoo formulations – efficacy, mechanism and test methods," *International Journal of Cosmetic Science*, vol. 22, no. 1, pp. 1-10, 2000, doi: <https://doi.org/10.1046/j.1467-2494.2000.00003.x>.
- [8] G. V. Scott, C. Robbins, and J. D. Barnhurst, "Sorption of quaternary ammonium surfactants by human hair," *Journal of the Society of Cosmetic Chemists*, vol. 20, pp. 135-152, 1969.
- [9] R. L. McMullen, D. Laura, G. Zhang, and B. Kroon, "Investigation of the interactions of cationic guar with human hair by electrokinetic analysis," *International Journal of Cosmetic Science*, vol. 43, no. 4, pp. 375-390, 2021, doi: 10.1111/ics.12704.
- [10] G. Ran, Y. Zhang, Q. Song, Y. Wang, and D. Cao, "The adsorption behavior of cationic surfactant onto human hair fibers," *Colloids and Surfaces B: Biointerfaces*, vol. 68, no. 1, pp. 106-110, 2009/1//2009, doi: 10.1016/j.colsurfb.2008.09.024.
- [11] G. Luengo, E. Guzman, L. Fernández-Peña, F. Leonforte, F. Ortega, and R. G. Rubio, "Interaction of polyelectrolytes and surfactants on hair surfaces. Deposits and their characterisation," in *Surface Science and Adhesion in Cosmetics*, K. L. Mittal and H. S. Bui Eds.: Scrivener Publishing LLC, 2021, ch. 13.
- [12] C. Bellmann, A. Synytska, A. Caspari, A. Drechsler, and K. Grundke, "Electrokinetic investigation of surfactant adsorption," *Journal of Colloid and Interface Science*, vol. 309, no. 2, pp. 225-230, 2007/5//2007, doi: 10.1016/j.jcis.2007.02.003.
- [13] M. A. Brown, T. A. Hutchins, C. J. Gamsky, M. S. Wagner, S. H. Page, and J. M. Marsh, "Liquid crystal colloidal structures for increased silicone deposition efficiency on colour-treated hair," *International Journal of Cosmetic Science*, vol. 32, no. 3, pp. 193-203, 2010, doi: 10.1111/j.1468-2494.2010.00540.x.

- [14] J. V. Gruber, B. R. Lamoureux, N. Joshi, and L. Moral, "The use of X-ray fluorescent spectroscopy to study the influence of cationic polymers on silicone oil depositio from shampoo," *Journal of Cosmetic Science*, vol. 52, pp. 131-136, 2001.
- [15] L. Labarre *et al.*, "Hair surface interactions against different chemical functional groups as a function of environment and hair condition," *Int J Cosmet Sci*, vol. 45, no. 2, pp. 224-235, Apr 2023, doi: 10.1111/ics.12834.
- [16] E. Guzman, F. Ortega, N. Baghdadli, C. Cazeneuve, G. S. Luengo, and R. G. Rubio, "Adsorption of conditioning polymers on solid substrates with different charge density," *ACS Appl Mater Interfaces*, vol. 3, no. 8, pp. 3181-8, Aug 2011, doi: 10.1021/am200671m.
- [17] T. Luxbacher, *The ZETA Guide, Principles of the streaming potential technique*, 1 ed. Graz: Anton Paar GmbH, 2014.
- [18] H. P. Tham *et al.*, "Influence of particle parameters on deposition onto healthy and damaged human hair," *International Journal of Cosmetic Science*, 2024.
- [19] "More than charge: The zeta potential reveals the adsorption of shampoo and conditioner on hair."
- [20] H. J. Jacobasch, K. Grundke, S. Schneider, and F. Simon, "Surface Characterization of Polymers by Physico-Chemical Measurements," *The Journal of Adhesion*, vol. 48, no. 1-4, pp. 57-73, 1995/01/01 1995, doi: 10.1080/00218469508028154.
- [21] S. Temmel, W. Kern, and T. Luxbacher, "Zeta Potential of Photochemically Modified Polymer Surfaces," in *Characterization of Polymer Surfaces and Thin Films*, Berlin, Heidelberg, K. Grundke, M. Stamm, and H.-J. Adler, Eds., 2006// 2006: Springer Berlin Heidelberg, pp. 54-61.
- [22] K. Stana-Kleinschek, T. Kreze, V. Ribitsch, and S. Strnad, "Reactivity and electrokinetical properties of different types of regenerated cellulose fibres," *Colloids and Surfaces A: Physicochemical and Engineering Aspects*, vol. 195, no. 1, pp. 275-284, 2001/12/30/ 2001, doi: [https://doi.org/10.1016/S0927-7757\(01\)00852-4](https://doi.org/10.1016/S0927-7757(01)00852-4)
- [23] E. Weiand *et al.*, "Effects of surfactant adsorption on the wettability and friction of biomimetic surfaces," *Phys Chem Chem Phys*, vol. 25, no. 33, pp. 21916-21934, Aug 23 2023, doi: 10.1039/d3cp02546b.
- [24] R. Zana, "Dimeric (Gemini) Surfactants: Effect of the Spacer Group on the Association Behavior in Aqueous Solution," *Journal of Colloid and Interface Science*, vol. 248, no. 2, pp. 203-220, 2002/04/15/ 2002, doi: <https://doi.org/10.1006/jcis.2001.8104>.
- [25] K. Yorke and S. Amin, "High Performance Conditioning Shampoo with Hyaluronic Acid and Sustainable Surfactants," *Cosmetics*, vol. 8, no. 3, p. 71, 2021. [Online]. Available: <https://www.mdpi.com/2079-9284/8/3/71>.
- [26] M. Minguet, N. Subirats, P. Castán, and T. Sakai, "Behenamidopropyl Dimethylamine: unique behaviour in solution and in hair care formulations," *International Journal of Cosmetic Science*, vol. 32, no. 4, pp. 246-257, 2010, doi: <https://doi.org/10.1111/j.1468-2494.2009.00566.x>.
- [27] R. Espinoza, "Multivesicular emulsion drug delivery systems," USA, 2004.
- [28] Y. S. Youn, "The Effect of Deposition Time on the Surface Coverage of Sublimation Deposited Solid-Phase Glycine and Proline Molecules Measured by Scanning Tunneling Microscopy," (in eng), *Molecules*, vol. 25, no. 13, Jun 28 2020, doi: 10.3390/molecules25132962.